GVB–RP: A Reliable MCSCF Wave Function for Large Systems

FRANCESCO FAGLIONI, WILLIAM A. GODDARD, III

Materials and Process Simulation Center, Beckman Institute (139-74), Division of Chemistry and Chemical Engineering, California Institute of Technology, Pasadena California 91125

Received 6 August 1998; accepted 4 December 1998

ABSTRACT: We have developed a version of generalized valence bond (GVB) that overcomes the major weakness of the perfect pairing approximation without requiring a full transformation of the integrals at each step of the self-consistent orbital optimization. The method, called generalized valence bond–restricted pairing (GVB–RP), describes properly the dissociation of up to triple bonds and provides smooth potential energy surfaces for most chemical reactions. The wave functions obtained are a good starting point for more sophisticated computational techniques. The applicability of the method is illustrated with a few simple examples including multiple-bond dissociations, transition states for symmetry allowed, symmetry forbidden, and radical reactions, as well as reactions at a transition-metal center. The cost of the method compares well with other self-consistent correlated techniques. © 1999 John Wiley & Sons, Inc. Int J Quant Chem 73: 1–22, 1999

Key words: ab initio; MCSCF; GVB; quantum chemistry; computational chemistry

Introduction

Accurate and reliable potential energy surfaces are essential for assessing chemical reaction rates and mechanisms. A common approach to compute ab initio energies is to start from the Hartree–Fock (HF) wave function (either restricted or unrestricted) and to correct the result with a number of standard methods to estimate the correlation energy. Such methods include partial configuration interaction (CI) expansions and perturbative treatments (e.g., second-order Møller–Plesset method).

This approach has two major shortcomings: (1) the correlation energy (i.e., the difference between the HF and the full CI energy for a given basis set) depends strongly on the nuclear position, being in general small close to equilibrium geometry and big as one or more bonds are stretched, broken,

Correspondence to: W. A. Goddard III.

Contract grant sponsor: NSF.

Contract grant numbers: ASC 92-17368; CHE95-22179.

Contract grant sponsors: ARO/DURIP; BP Chemical; ARO; Exxon; Seiko-Epson; Owens Corning; Asahi Chemical, Saudi Aramco; Beckman Institute; Chevron Petroleum Technology Co.; Chevron Chemical Co., NASA/Ames; NASA/JPL; ONR; Avery Dennison; Chevron Research Technology Co.

CCC 0020-7608 / 99 / 010001-22

and reformed. The post-HF corrections, therefore, need to be accurate and expensive in order to correctly describe the regions where the correlation energy is big. (2) Near the transition states for forbidden reactions, the HF potential energy corresponding to a given spin state contains nonphysical edges (discontinuities in the gradient). This problem generally remains for the higher level treatments.

A convenient way to handle these problems is to use as starting point for the correlation treatment a better self-consistent wave function, including just enough correlation to correctly describe bond dissociations and transition states. Several multiconfiguration self-consistent field (MCSCF) wave function [1, 2] are appropriate, ranging from a simple one-pair generalized valence bond (GVB) calculation for a single-bond dissociation to larger complete active-space self-consistent field (CASSCF) [3] for more complicated systems. In general, including additional configurations in the self-consistent field (SCF) is more expensive. It is therefore important to select a wave function that has just the right amount of correlation.

The GVB–PP (generalized valence bond with perfect pairing approximation) [4, 5] wave function is excellent in describing reactions involving breaking and formation of single bonds, as it does not require expensive integral transformations at each step of the SCF procedure. GVB–PP, however, has similar problems to HF in describing multiple bonds and forbidden reactions. More general forms of GVB [5], as well as most other forms of MCSCF [1–3] (including CASSCF), require a complete transformation of the four center integrals at each step of the SCF, making the cost increase very rapidly with the size of the system.

Here we present a method to obtain self-consistent wave functions at a level that is intermediate between the most general GVB and the GVB–PP. The method, called GVB–RP (GVB with the restricted pairing approximation), is the self-consistent version of GVB–RCI (GVB–PP followed by restricted configuration interaction) [6] and includes the minimum number of configurations to correctly describe dissociation for up to triple bonds and transition states involving few electrons. Although the same approach can be generalized to arbitrary bond order and number of electrons, the current version should be able to describe properly most of the interesting molecules that require going beyond HF or GVB–PP wave functions but are too big for CASSCF treatments. Because of the very limited number of configurations included, only a partial integral transformation is required at each self-consistent step. The cost of the method scales well with the size of the system, making this approach promising for future applications to extensive systems.

The next section outlines the method and derives the main formulas used. The third section reports results obtained for simple reactions and compares them with other computational methods.

Theoretical Method

FORMALISM

We use lowercase letters $a, b, \ldots, i, j, \ldots$ to indicate orthogonal orbitals. The orbitals in the GVB space (or *active* orbitals) are grouped into pairs. The two orbitals of each pair are denoted as g for the bonding orbital (good) and u for the antibonding orbital (ungood), which does not imply that the pair has symmetry (both orbitals can have the same symmetry). We use capital letters to indicate the pair number; for instance, g_I indicates the g orbital of pair I. The symbol C indicates a numerical coefficient.

GVB–PP WAVE FUNCTION

The GVB–PP wave function describes each pair of active electrons with two variationally optimized overlapping (i.e., nonorthogonal) orbitals:

$$\Psi^{\mathrm{GVB}} = [\phi_a(1)\phi_b(2) + \phi_b(1)\phi_a(2)](\alpha\beta - \beta\alpha).$$

Nonactive orbitals are treated as doubly occupied (as in the HF level) or high spin open shell.

It is convenient to carry out the GVB computations in terms of orthogonal orbitals, obtained by rewriting each GVB pair in the natural orbital representation:

$$\Psi^{\mathrm{NO}} = [C^g gg - C^u uu](\alpha\beta - \beta\alpha).$$

Thus, GVB–PP wave function has the form

$$\Psi^{\mathrm{GVB-PP}} = [\{\mathrm{core}\}\{\mathrm{open}\}\Psi^{\mathrm{NO}}(1,2)\Psi^{\mathrm{NO}}(3,4)\ldots], \quad (1)$$

where {core} and {open} are products of restricted HF (RHF)-like orbitals with double and single occupancy, respectively. All singly occupied orbitals

are assumed to have spin α. This is a special case of the full GVB wave function, since the full GVB wave function allows all possible spin couplings of the active orbitals, whereas Eq. (1) has just a single valence bond (or perfect pairing) coupling of the spins. The GVB–PP wave function builds in *static correlation* between electrons in each GVB pair, by allowing them to each occupy their own orbital, on the average staying farther apart from one another than if they were restricted to occupy the same spatial orbital.

Upon homolytic bond dissociation, the two electrons forming the bond can smoothly follow the two fragments as they separate. However, for multiple bonds the optimal wave function should generally dissociate to two high spin fragments, but GVB–PP forces each electron within a pair to have equal probability of having spin α or β, regardless of the spin in the other bond pairs. Consequently, GVB–PP leads to a mixture of high and low spin components. Generally, previous GVB calculations for dissociation of multiple bonds used the GVB–PP representation but added a full CI among the GVB orbitals (GVB–CI). This includes the proper spin configuration and generally leads to a good dissociation. In some cases, GVB3 was used to optimize the orbital for the GVB–CI wave function, leading to proper dissociation. An efficient alternative was the correlation consistent CI method (CC–CI) which incorporates all correlations that directly affect the bond dissociation.

For reactions in which pairs of electrons must exchange partners, GVB–PP often cannot do the exchange smoothly, leading to cusps in potential energy surface. Again this can be handled with GVB–CI or CC–CI but at some loss in interpretation.

GVB–RP

In order to overcome the weakness of GVB–PP, it is necessary to include configurations to allow electrons in different GVB pairs to be singlet paired and hence electrons within the same GVB pair to be triplet paired. The simplest way to do this is to include configurations where two separate GVB pairs have their spins coupled into a triplet while the overall spin state (for the two GVB pairs) remains a singlet (the GF spin coupling in the original SOGI version of GVB theory).

To describe the resulting wave function, we define the following intermediate symbols to indicate GVB pairs and restricted pairing groups of four orbitals from two GVB pairs:

$$(\mathrm{GVB})_I = (C_I^g g_I g_I - C_I^u u_I u_I)\Theta_1, \qquad (C_I^g)^2 + (C_I^u)^2 = 1, \tag{2}$$

$$(\mathrm{RP})_{IJ} = (g_I u_I g_J u_J)\Theta_2(C_{IJ}^s, C_{IJ}^t), \qquad (C_{IJ}^s)^2 + (C_{IJ}^t)^2 = 1, \tag{3}$$

where the spin functions Θ are

$$\begin{aligned}
\Theta_1 &= \frac{1}{\sqrt{2}}(\alpha\beta - \beta\alpha),\\
\Theta_2 &= \frac{C_{IJ}^s}{2}(\alpha\beta - \beta\alpha)(\alpha\beta - \beta\alpha)\\
&\quad + \frac{C_{IJ}^t}{\sqrt{12}}[2\alpha\alpha\beta\beta + 2\beta\beta\alpha\alpha\\
&\quad - (\alpha\beta + \beta\alpha)(\alpha\beta + \beta\alpha)]\\
&= \frac{C_{IJ}^t}{\sqrt{3}}(\alpha\alpha\beta\beta + \beta\beta\alpha\alpha)\\
&\quad + \left(\frac{C_{IJ}^s}{2} - \frac{C_{IJ}^t}{\sqrt{12}}\right)(\alpha\beta\alpha\beta + \beta\alpha\beta\alpha)\\
&\quad - \left(\frac{C_{IJ}^s}{2} + \frac{C_{IJ}^t}{\sqrt{12}}\right)(\alpha\beta\beta\alpha + \beta\alpha\alpha\beta).
\end{aligned}$$

It is also convenient to define the following terms:

$$\begin{aligned}
\Psi^{\mathrm{PP}} &= |\{\mathrm{core}\}(\mathrm{GVB})_1 \ldots (\mathrm{GVB})_n\rangle,\\
\Psi_{12}^{\mathrm{RP}} &= |\{\mathrm{core}\}(\mathrm{RP})_{12}(\mathrm{GVB})_3 \ldots (\mathrm{GVB})_n\rangle,\\
\Psi_{IJ}^{\mathrm{RP}} &\quad \text{by analogy with } \Psi_{12}^{\mathrm{RP}},
\end{aligned}$$

where Ψ^{PP} has the form of a traditional GVB–PP wave function, Ψ_{IJ}^{RP} represents the same wave function where two electrons from pairs I and J have had their spins recoupled. Since in Ψ_{IJ}^{RP} the four electrons from pairs I and J occupy four different orbitals, we only require that the overall spin state is a singlet.

The GVB–RP wave function with RP correlation on N_r GVB pairs is

$$\Psi = C_0\Psi^{\mathrm{PP}} + \sum_{I,J>I}^{N_r} C_{IJ}\Psi_{IJ}^{\mathrm{RP}}, \qquad C_0^2 + \sum_{I,J>I}^{N_r} (C_{IJ})^2 = 1. \tag{4}$$

It is convenient to define

$$C_{II} = 0, \qquad C_{JI} = C_{IJ}$$

so that Eq. (4) can be rewritten as

$$\Psi = C_0\Psi^{\mathrm{PP}} + \tfrac{1}{2}\sum_{I,J}^{N_r} C_{IJ}\Psi_{IJ}^{\mathrm{RP}}, \qquad C_0^2 + \tfrac{1}{2}\sum_{I,J}^{N_r}(C_{IJ})^2 = 1. \tag{5}$$

We also define the *perfect pairing density* for pair I as

$$\Gamma_I = 1 - \sum_J C_{IJ}^2,$$

where Γ_I is a measure of the importance of the PP coupling within pair I. If pair I is not included in the RP treatment, then all coefficients C_{IJ} are null and $\Gamma_I = 1$.

TOTAL ENERGY

The energy associated with wave function (5) is

$$\begin{aligned} E = &\sum_i 2f_i h_i + \sum_{i,j}(a_{ij}J_{ij} + b_{ij}K_{ij}) \\ &+ \sum_{I,J}[\, r_{IJ}(g_I g_J|u_I u_J) \\ &+ s_{IJ}(g_I u_J|u_I g_J) + t_{IJ}(g_I u_I|g_J u_J)], \end{aligned} \tag{6a}$$

where f is given by

$$\begin{aligned} &f_i = 1, && \text{if } i \text{ is a core orbital;} \\ &f_i = \tfrac{1}{2}, && \text{if } i \text{ is an open shell orbital;} \\ &f_i = \Gamma_I C_i^2 + \tfrac{1}{2}(1-\Gamma_I), \\ &&& \text{if } i \in I \text{ where } I \text{ is a GVB pair.} \end{aligned} \tag{6b}$$

The a_{ij} and b_{ij} are given by

$$a_{ij} = 2f_i f_j, \qquad b_{ij} = -f_i f_j \tag{6c}$$

except that (i) if i and j are both open shell orbitals, then

$$b_{ij} = -\tfrac{1}{2};$$

(ii) if i is a pair orbital, then

$$\begin{cases} a_{ii} = \Gamma_I C_i^2, \\ b_{ii} = 0; \end{cases}$$

(iii) if i and j are in the same pair I, then

$$\begin{cases} a_{ij} = \tfrac{1}{2}(1-\Gamma_I), \\ b_{ij} = -\Gamma_I C_i C_j - \tfrac{1}{2}\sum_J C_{IJ}^2\left[(C_{IJ}^t)^2 - (C_{IJ}^s)^2\right]; \end{cases}$$

(iv) if $i \in I$, $j \in J \neq I$ and $I, J \in \mathrm{RP}$, then

$$\begin{aligned} a_{ij} = (\Gamma_I + \Gamma_J + C_{IJ}^2 - 1)2C_i^2 C_j^2 + (1 - \Gamma_I - C_{IJ}^2)C_j^2 \\ + (1 - \Gamma_J - C_{IJ}^2)C_i^2 + \tfrac{1}{2}C_{IJ}^2; \end{aligned}$$

(v) if $i, j \in \mathrm{RP}$ with $|i-j|$ even, then

$$\begin{aligned} b_{ij} = &-(\Gamma_I + \Gamma_J + C_{IJ}^2 - 1)C_i^2 C_j^2 \\ &-\tfrac{1}{2}(1 - \Gamma_I - C_{IJ}^2)C_j^2 \\ &-\tfrac{1}{2}(1 - \Gamma_J - C_{IJ}^2)C_i^2 \\ &- C_{IJ}^2\left\{\tfrac{1}{4}\left[(C_{IJ}^s)^2 - (C_{IJ}^t)^2\right] - \frac{\sqrt{3}}{2}C_{IJ}^s C_{IJ}^t\right\}, \end{aligned}$$

(vi) if $i, j \in \mathrm{RP}$ with $|i-j|$ odd, then

$$\begin{aligned} b_{ij} = &-(\Gamma_I + \Gamma_J + C_{IJ}^2 - 1)C_i^2 C_j^2 \\ &-\tfrac{1}{2}(1 - \Gamma_I - C_{IJ}^2)C_j^2 \\ &-\tfrac{1}{2}(1 - \Gamma_J - C_{IJ}^2)C_i^2 \\ &- C_{IJ}^2\left\{\tfrac{1}{4}\left[(C_{IJ}^s)^2 - (C_{IJ}^t)^2\right] + \frac{\sqrt{3}}{2}C_{IJ}^s C_{IJ}^t\right\}. \end{aligned}$$

The r_{IJ}, s_{IJ}, and t_{IJ} are given by

$$\begin{aligned} r_{IJ} = &C_0 C_{IJ}(C_I^g C_J^u + C_I^u C_J^g)\left(\sqrt{3}\,C_{IJ}^t + C_{IJ}^s\right) \\ &-(C_I^g C_J^g + C_I^u C_J^u) \\ &\times \sum_K C_{IK}C_{JK}(C_{IK}^s C_{JK}^s + C_{IK}^t C_{JK}^t), \\ s_{IJ} = &C_0 C_{IJ}(C_I^g C_J^g + C_I^u C_J^u)\left(\sqrt{3}\,C_{IJ}^t - C_{IJ}^s\right) \\ &+(C_I^g C_J^u + C_I^u C_J^g) \\ &\times \sum_K C_{IK}C_{JK}(C_{IK}^s C_{JK}^s - C_{IK}^t C_{JK}^t), \\ t_{IJ} = &C_0 C_{IJ}(C_I^g - C_I^u)(C_J^g - C_J^u)(2C_{IJ}^s) \\ &+(C_I^g - C_I^u)(C_J^g - C_J^u)\sum_K C_{IK}C_{JK}(2C_{IK}^s C_{KJ}^s). \end{aligned} \tag{6d}$$

If I or J are treated at the PP level, then these reduce to $r_{IJ} = s_{IJ} = t_{IJ} = 0$.

We can express the energy in a more standard form:

$$E = \sum_i 2f_i h_i + \sum_{i,j,k,l} c_{ijkl}(ij|kl), \tag{7a}$$

where the f are all zero, except

$$\begin{aligned} f_i &= 1, && \text{if } i \text{ is a core orbital;} \\ f_i &= \tfrac{1}{2}, && \text{if } i \text{ is an open orbital;} \\ f_i &= \Gamma_I C_i^2 + \tfrac{1}{2}(1-\Gamma_I), && \text{if } i \in I; \end{aligned} \tag{7b}$$

and c_{ijkl} are all zero, except

$$\begin{aligned} c_{iiii} &= a_{ii} + b_{ii}, \\ c_{iijj} &= a_{ij}, \\ c_{ijij} &= c_{ijji} = b_{ij}/2, \\ c_{ijkl} &= r_{IJ}/4 \quad \text{if} \begin{cases} i,k \in I \in \text{RP and} \\ \quad j,l \in J \in \text{RP with} \\ \quad I \neq J \text{ and} \\ \quad (k-i) = (l-j), \\ i,l \in I \in \text{RP and} \\ \quad j,k \in J \in \text{RP with} \\ \quad I \neq J \text{ and} \\ \quad (l-i) = (k-j), \end{cases} \\ c_{ijkl} &= s_{IJ}/4 \quad \text{if} \begin{cases} i,k \in I \in \text{RP and} \\ \quad j,l \in J \in \text{RP with} \\ \quad I \neq J \text{ and} \\ \quad (k-i) \neq (l-j), \\ i,l \in I \in \text{RP and} \\ \quad j,k \in J \in \text{RP with} \\ \quad I \neq J \text{ and} \\ \quad (l-i) \neq (k-j), \end{cases} \\ c_{ijkl} &= t_{IJ}/4 \quad \text{if } i,j \in I \in \text{RP and} \\ &\qquad\quad k,l \in J \in \text{RP with } I \neq J. \end{aligned} \tag{7c}$$

ORBITAL OPTIMIZATION

To minimize the energy of an initial guess wave function with respect to orbital shapes and CI coefficients, we need to estimate the effect of rotations between orbitals and between CI coefficients. For a self-consistent optimization algorithm, it is only necessary to estimate the effects of such rotations one at the time. In particular, we can optimize the CI coefficients for a given set of orbitals, then improve the orbitals assuming the CI coefficients are fixed and iterate to convergence.

General MCSCF Treatment

To optimize the shape of the orbitals, we consider all possible pairwise rotations, assuming that they are independent.

The new (improved) orbitals $|\phi'\rangle$ are obtained by a unitary transformation T of the old orbitals $|\phi\rangle$. The transformation matrix is written as

$$\mathbf{T} = \exp(\mathbf{\Delta}),$$

where $\mathbf{\Delta}$ is an antisymmetric matrix containing the rotation angles between the orbitals.

We optimize the rotation angles variationally, assuming that all rotations are independent. The angle Δ_{pq} must satisfy the condition

$$\frac{\partial E}{\partial \Delta_{pq}} = 0. \tag{8}$$

Upon application of the rotation

$$|\phi'_r\rangle = \sum_i T_{ri} |\phi_i\rangle,$$

the energy expression (7) transforms as follows:

$$\begin{aligned} E' &= \sum_r 2 f_r \langle \phi'_r | h | \phi'_r \rangle + \sum_{rstu} c_{rstu} (\phi'_r \phi'_s | \phi'_t \phi'_u) \\ &= \sum_r 2 f_r \sum_{ij} T_{ri} T_{rj} \langle i | h | j \rangle \\ &\quad + \sum_{rstu} c_{rstu} \sum_{ijkl} T_{ri} T_{sj} T_{tk} T_{ul} (ij|kl). \end{aligned} \tag{9}$$

The energy dependence from the rotation Δ_{pq} and its derivative are

$$\begin{aligned} E(\Delta_{pq}) &= E_0 + \left(\frac{\partial E}{\partial \Delta_{pq}} \right)_{\Delta_{pq}=0} \Delta_{pq} \\ &\quad + \frac{1}{2} \left(\frac{\partial^2 E}{\partial \Delta_{pq}^2} \right)_{\Delta_{pq}=0} \Delta_{pq}^2 + \cdots \end{aligned} \tag{10}$$

$$\frac{\partial E}{\partial \Delta_{pq}} = \left(\frac{\partial E}{\partial \Delta_{pq}} \right)_{\Delta_{pq}=0} + \left(\frac{\partial^2 E}{\partial \Delta_{pq}^2} \right)_{\Delta_{pq}=0} \Delta_{pq} + \cdots \tag{11}$$

We estimate the optimal rotation angle by truncation of the series (11) at the second term and imposing condition (8), obtaining

$$\frac{\partial E}{\partial \Delta_{pq}} = 0 \Rightarrow \Delta_{pq} = -\left(\frac{\partial^2 E}{\partial \Delta_{pq}^2} \right)^{-1}_{\Delta_{pq}=0} \left(\frac{\partial E}{\partial \Delta_{pq}} \right)_{\Delta_{pq}=0}.$$

For simplicity we define

$$A_{pq} = \frac{1}{4}\left(\frac{\partial E}{\partial \Delta_{pq}}\right)_{\Delta_{pq}=0}, \qquad B_{pq} = \frac{1}{4}\left(\frac{\partial^2 E}{\partial \Delta_{pq}^2}\right)_{\Delta_{pq}=0}$$

so that the estimate for the optimal rotation is

$$\Delta_{pq} = -\frac{A_{pq}}{B_{pq}}.$$

Noticing that

$$(T_{rs})_{\mathbf{T}=\mathbf{I}} = \delta_{rs}, \tag{12}$$

$$\left(\frac{\partial T_{rs}}{\partial \Delta_{pq}}\right)_{\mathbf{T}=\mathbf{I}} = \delta_{rp}\delta_{sq} - \delta_{rq}\delta_{sp}, \tag{13}$$

$$\left(\frac{\partial^2 T_{rs}}{\partial \Delta_{pq}^2}\right)_{\mathbf{T}=\mathbf{I}} = -\delta_{pr}\delta_{ps} - \delta_{qr}\delta_{qs}, \tag{14}$$

we can evaluate A_{pq} and B_{pq} by direct differentiation of expression (9) and substitution of (12), (13), and (14). The result is

$$A_{pq} = f_p h_{qp} - f_q h_{pq} + \sum_{jkl}\left[c_{pjkl}(qj|kl) - c_{qjkl}(pj|kl)\right], \tag{15}$$

$$\begin{aligned} B_{pq} = {} & (f_q - f_p)(h_{pp} - h_{qq}) \\ & + \sum_{ijk}\left[-c_{pijk}(pi|jk) - c_{qijk}(qi|jk)\right] \\ & + \sum_{ij}\left[c_{ppij}(qq|ij) - c_{pqij}(qp|ij)\right. \\ & - c_{qpij}(pq|ij) + c_{qqij}(pp|ij) \\ & + c_{pipj}(qi|qj) - c_{piqj}(qi|pj) \\ & - c_{qipj}(pi|qj) + c_{qiqj}(pi|pj) \\ & + c_{pijp}(qi|jq) - c_{pijq}(qi|jp) \\ & \left. - c_{qijp}(pi|jq) + c_{qijq}(pi|jp)\right]. \end{aligned} \tag{16}$$

Specialization to GVB–RP

In the case of GVB–RP, the only nonzero coefficients in expression (7a) are given by (7c).

The energy can be expressed as

$$E = \sum_{i}^{\mathrm{occ}} 2 f_i h_i + \sum_{i,j}^{\mathrm{occ}} (a_{ij}J_{ij} + b_{ij}K_{ij}) + \sum_{i\neq j\neq k\neq l}^{\mathrm{RP}} c_{ijkl}(ij|kl),$$

and the variational principle imposes

$$\delta E = 4\sum_{i}^{\mathrm{occ}} \langle \delta\phi_i | f_i h + \sum_{j}^{\mathrm{occ}} (a_{ij}J_j + b_{ij}K_j)|\phi_i\rangle + 4\sum_{i\neq j\neq k\neq l}^{\mathrm{RP}} c_{ijkl}\left(\delta\phi_i\phi_j|\phi_k\phi_l\right).$$

In this case we can no longer define a Fock operator in terms of Coulomb and exchange operators because of the four index summation in the energy expression.

Although it is still possible to define a Fock operator in terms of one electron integral operators [2], this would contain a double summation over the active space. We prefer instead to use the GVB–PP Fock operators to simplify these expressions and add the corrective terms one case at a time.

We define the GVB–PP Fock operator for orbital i as

$$F^i = f_i h + \sum_{j}^{\mathrm{occ}} (a_{ij}J_j + b_{ij}K_j)$$

(but its self-consistent eigenfunctions do not minimize the energy).

In order to reduce the summation over the active space to a single index, we adopt the following formalism: if orbital p belongs to pair P ($p \in P$), then we call p' its partner (i.e., $p' \in P$; $p' \neq p$). Referring to another pair I, we call i and i' the two orbitals in the pair with the same position (g or u) as p and p', respectively.

The terms A_{pq} and B_{pq} originally described in (15) and (16) reduce to the following cases:

- If $p, q \notin \mathrm{RP}$, then

  $$A_{pq} = \langle p|F^p - F^q|q\rangle,$$
  $$B_{pq} = \langle p|F^q - F^p|p\rangle + \langle q|F^p - F^q|q\rangle + \gamma_{pq},$$

  where $\gamma_{pq} = 2(a_{pp} + a_{qq} - 2a_{pq})K_{pq} + (b_{pp} + b_{qq} - 2b_{pq})(K_{pq} + J_{pq})$.
- If $p \in \mathrm{RP}$ and $q \notin \mathrm{RP}$, then

  $$\begin{aligned} A_{pq} &= -A_{qp} \\ &= \langle p|F^p - F^q|q\rangle \\ &\quad + \tfrac{1}{2}\sum_{I(\neq P)}^{\mathrm{RP}} [t_{PI}(qp'|ii') + r_{PI}(qi|p'i') \\ &\quad + s_{PI}(qi'|p'i)], \end{aligned}$$

$$
\begin{aligned}
B_{pq} &= B_{qp} \\
&= \langle p|F^q - F^p|p\rangle \\
&\quad + \langle q|F^p - F^q|q\rangle + \gamma_{pq} \\
&\quad - \tfrac{1}{2}\sum_{I(\neq P)}^{\mathrm{RP}} [\, t_{PI}(pp'|ii') + r_{PI}(pi|p'i') \\
&\quad + s_{PI}(pi'|p'i)].
\end{aligned}
$$

- If $p \in P \in \mathrm{RP}$ and $q \in Q \in \mathrm{RP}$, then

$$
\begin{aligned}
A_{pq} &= \langle p|F^p - F^q|q\rangle \\
&\quad + \tfrac{1}{2}\sum_{I(\neq P)}^{\mathrm{RP}} [\, t_{PI}(qp'|ii') + r_{PI}(qi|p'i') \\
&\quad + s_{PI}(qi'|p'i)] \\
&\quad - \tfrac{1}{2}\sum_{I(\neq Q)}^{\mathrm{RP}} \big[\, t_{QI}(pq'|ii') + r_{QI}(pi|q'i') \\
&\quad + s_{QI}(pi'|q'i)\big].
\end{aligned}
$$

If $q \neq p'$, then B is

$$
\begin{aligned}
B_{pq} &= \langle p|F^q - F^p|p\rangle \\
&\quad + \langle q|F^p - F^q|q\rangle + \gamma_{pq} \\
&\quad - \tfrac{1}{2}\sum_{I(\neq P)}^{\mathrm{RP}} [\, t_{PI}(pp'|ii') + r_{PI}(pi|p'i') \\
&\quad + s_{PI}(pi'|p'i)] \\
&\quad - \tfrac{1}{2}\sum_{I(\neq Q)}^{\mathrm{RP}} \big[\, t_{QI}(qq'|ii') + r_{QI}(qi|q'i') \\
&\quad + s_{QI}(qi'|q'i)\big] \\
&\quad - r_{PQ}(pq|p'q') - s_{PQ}(pp'|qq') \\
&\quad - t_{PQ}(pq'|p'q),
\end{aligned}
$$

while in the special case that $q = p'$

$$
\begin{aligned}
B_{pq} &= \langle p|F^q - F^p|p\rangle \\
&\quad + \langle q|F^p - F^q|q\rangle + \gamma_{pq} + \\
&\quad - \tfrac{1}{2}\sum_{I(\neq P)}^{\mathrm{RP}} [4t_{PI}(pp'|ii') \\
&\quad + (3r_{PI} + s_{PI})(pi|p'i') \\
&\quad + (r_{PI} + 3s_{PI})(pi'|p'i)].
\end{aligned}
$$

- If $p \notin \mathrm{RP}$ and q is virtual, then

$$
\begin{aligned}
A_{pq} &= -A_{qp} = \langle p|F^p|q\rangle, \\
B_{pq} &= B_{qp} = \langle q|F^p|q\rangle - \langle p|F^p|p\rangle \\
&\quad + 2a_{pp}K_{pq} + b_{pp}(K_{pq} + J_{pq}).
\end{aligned}
$$

- If $p \in \mathrm{RP}$ and q is virtual, then

$$
\begin{aligned}
A_{pq} &= -A_{qp} \\
&= \langle p|F^p|q\rangle + \tfrac{1}{2}\sum_{I(\neq P)}^{\mathrm{RP}} [\, t_{PI}(qp'|ii') \\
&\quad + r_{PI}(qi|p'i') + s_{PI}(qi'|p'i)], \\
B_{pq} &= B_{qp} \\
&= \langle q|F^p|q\rangle - \langle p|F^p|p\rangle \\
&\quad + 2a_{pp}K_{pq} + b_{pp}(K_{pq} + J_{pq}) \\
&\quad - \tfrac{1}{2}\sum_{I(\neq P)}^{\mathrm{RP}} [\, t_{PI}(pp'|ii') + r_{PI}(pi|p'i') \\
&\quad + s_{PI}(pi'|p'i)].
\end{aligned}
$$

Integral Requirements

The GVB–PP calculation requires the computation of one-electron terms and the two-electron operators J and K for all occupied orbitals. The GVB–RP requires the additional effort of computing the four-orbital integrals $(pq|ii')$, $(pi|qi')$, and $(pi'|qi)$ where $p \in \mathrm{RP}$, $i, i' \in I \in \mathrm{RP}$, and q is any orbital (occupied or virtual).

In the general case of N orbitals and R GVB pairs involved in the RP correlation ($2R$ orbitals). the extra cost is readily estimated as follows:

$$
\begin{aligned}
\text{extra cost} = {} & \underset{3}{\text{integral types}} * \underset{N}{q \text{ range}} \\
& * \underset{R}{i, i' \text{ range}} * \underset{2(R-1)}{p \text{ range}}
\end{aligned}
$$

so the overall extra cost due to integral computations is:

$$\text{extra cost} = 6NR(R-1)$$

OPTIMIZATION OF CI COEFFICIENTS

Assuming the orbitals are frozen, the optimization of the CI coefficients can exploit all the pairwise constraint relations forced upon the coefficients by the energy expression.

In the current implementation, we optimize all the CI coefficients at each wave function iteration,

with the following procedure. First, all the pair coefficients are optimized self-consistently, then the spin coupling coefficients, then the CI coefficients. We repeat the cycle until all the coefficients are stable and consistent with one another.

The derivation of detailed formulas to carry out the optimization is tedious but involves no new techniques or ideas. The detailed formulas used are included in the appendix.

Applications

DISSOCIATION OF MULTIPLE BONDS

We examined the dissociation of the diatomic molecules N_2 and CO. For each molecule we studied the dissociation potential energy profiles at various levels of theory, using the 6-31G* basis set.

N_2 Molecule

The results for the dissociation of N_2 are summarized in Figure 1. As expected, RHF gives a poor description of the bond and the wrong dissociation limit. RHF gives also a bad wave function for the MP2 treatment, as testified by the restricted MP2 (RMP2) curve in Figure 1. At the next level of theory, the unrestricted HF (UHF) predicts a barrier of about 9.3 kcal/mol for the formation of the molecule. The MP2 treatment of the UHF [unrestricted MP2 (UMP2)] wave function reduces the barrier to about 1.2 kcal/mol, but it fails to eliminate it. Also, UMP2 predicts an edge close the the equilibrium geometry which is not physical.

At the GVB–PP level, the triple-bond formation is barrierless, but the dissociation limit is not the ground state, as the two fragments are not in their high spin configurations. This leads to a dissociate limit 66.7 kcal/mol above the correct limit. Re-

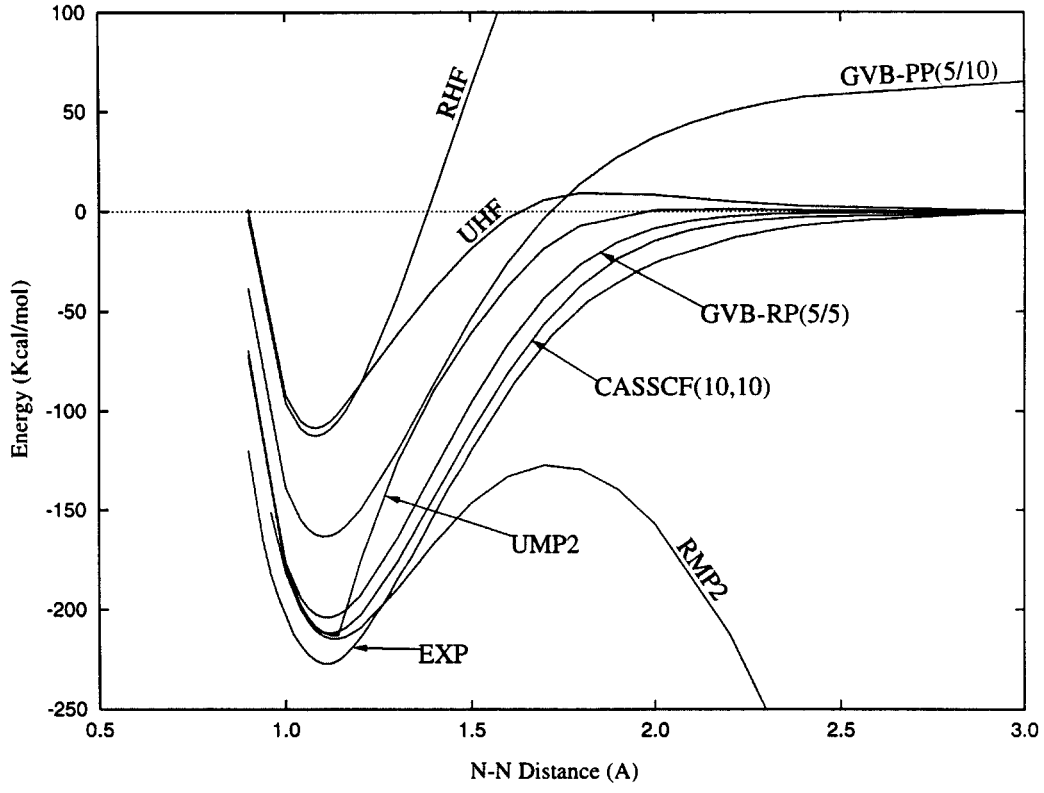

FIGURE 1. N_2 dissociation potential at various levels of theory (all using 6-31G* basis sets). RMP2 and UMP2 refer to the MP2 treatment on top of RHF and UHF, respectively. GVB–PP(N/M) indicates GVB–PP correlation on N pairs comprising a total of M orbitals. In the case of two orbitals per pair $M = 2N$. GVB–RP(N/M) indicates RP correlation on N pairs out of M and PP correlation on the remaining (M–N). CASSCF(N, M) indicates an active space containing N electrons and M orbitals. The experimental curve [7] is included for comparison.

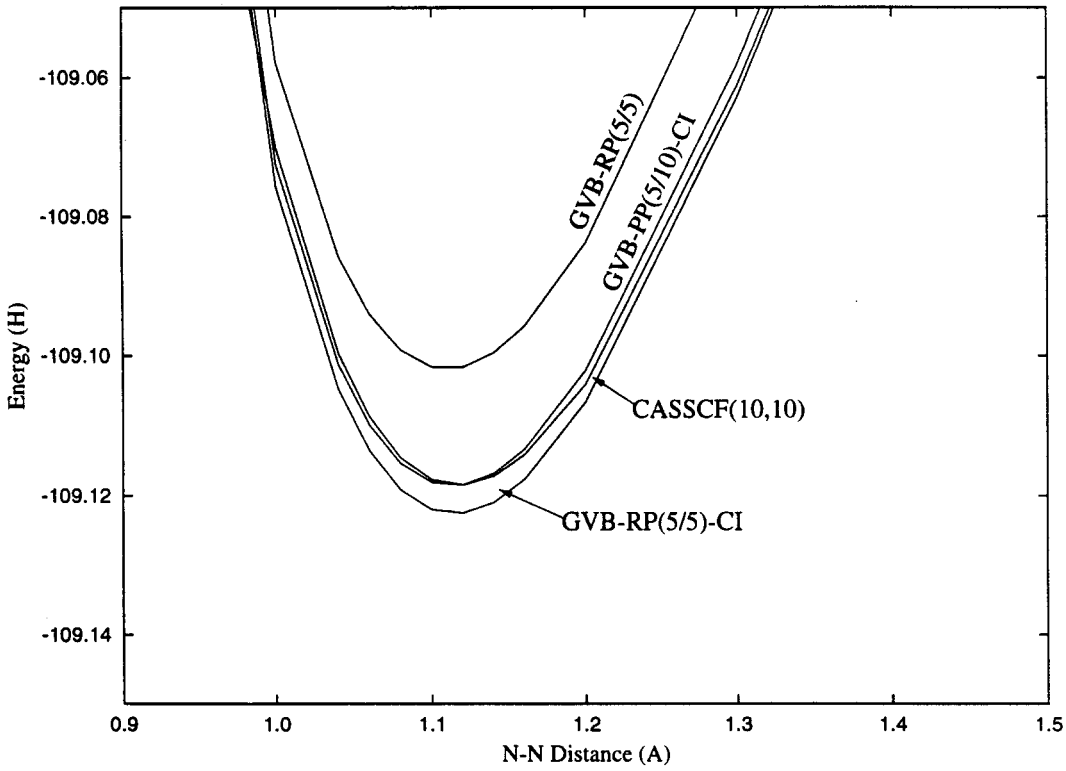

FIGURE 2. Equilibrium region of the N_2 potential at various levels of theory (all using 6-31G* basis sets). GVB–RP and CASSCF are self-consistent. GVB–PP + CI and GVB–RP + CI are active-space CI based on GVB–PP and GVB–RP wave functions, respectively. The fact that CASSCF gives higher energy than GVB–RP + CI is due to the inability of the commercial implementation of CASSCF used to select the best active orbitals.

stricted HF leads to a limit approximately 700 kcal/mol above the dissociate limit.

Both GVB-RP(5/5) and CASSCF(10, 10) give a more realistic potential energy profile. The experimental energy [7] is reported for comparison.

To compare the active space provided by various methods, we performed a complete active-space CI on top of the GVB–PP and GVB–RP wave functions. The results are reported in Figure 2. Notice that the commercial version of CASSCF used fails to identify the best active space for this system, missing part of the correlation between $2s$ electrons on the same nitrogen atom. The computed bond energies are reported in Table I.

CO Molecule

The results obtained for the CO molecule are summarized in Figure 3. While in this case the UHF result is qualitatively correct, the GVB–RP treatment gives a substantially better result approaching the CASSCF quality.

Figure 4 shows that the GVB–RP active space is close to optimal for a broad region around the

TABLE I
Computed bond energies of N_2 and CO in kcal / mol.

Bond	UHF	UHF + MP2	GVB–PP	GVB–RP	CASSCF	Exper.
N_2	108.7	212.7	163.3[a]	203.9[a]	211.8[a]	228.5
CO	171.7	255.2	207.8[b]	244.2[b]	253.0[b]	257.3

[a] Indicates 10 electrons, 10 orbitals active space, corresponding to 5 GVB pairs.
[b] Indicates 6 electrons, 6 orbitals active space, corresponding to 3 GVB pairs.

equilibrium geometry. Although CASSCF is preferable for the stretched bond (between 1.7 and 2.3 Å), it does not select the optimal active space at distances larger than 2.5 Å. The computed bond energies are reported in Table I.

TRANSITION STATES

Radical Reaction: $H_2 + H$

The simplest reaction we studied is the linear $H_2 + H \rightarrow H + H_2$. The results for several levels of computations are reported in Figure 5. To have an even number of electrons in the active space, the unpaired electron was formally paired with a fourth electron placed on a hydrogen atom at infinite distance.

In this case UHF, GVB–RP, and CASSCF all provide reasonable descriptions of the reaction. RHF and GVB–PP predict an unphysical edge at the transition state. The edge is due to the restricted or the perfect pairing nature of the wave function: At the transition state the electrons cannot rearrange the pairing in a smooth way unless more than two natural orbitals per pair are allowed. The full CI energy profile indicates that post-SCF treatment is required to account for a significant portion of the correlation energy.

The reaction coordinate was computed at various levels or theory, and the results for the saddle point region are reported in Figure 6. The full CI energy profile was computed at CASSCF geometries. Only the transition-state geometry was optimized at the full CI level, and the result is included in Figure 6 for comparison. GVB–RP provides essentially the same geometry as CASSCF for the maximum along the reaction coordinate while UHF and GVB–PP predict bond lengths shorter by 0.036 Å.

Allowed Reaction: $H_2 + H_2 + H_2$

As an example of allowed reaction, we studied the three molecular $H_2 + H_2 + H_2$ with D_{3h} (hexagonal planar) geometry. The reaction coordinate was determined at the MP2 level with 6-31G** basis set. The same reaction coordinate and basis set was used for all levels of theory.

The reaction profiles are reported in Figure 7. In this case all the methods considered provide a

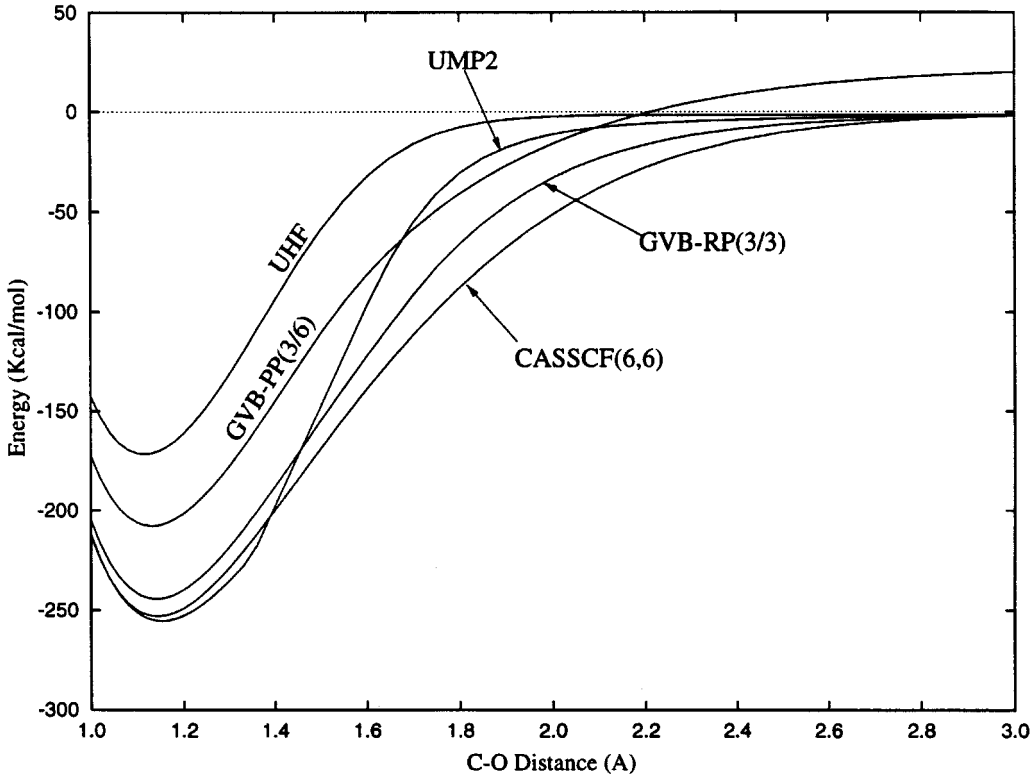

FIGURE 3. CO dissociation potential at various levels of theory (all using the 6-31G* basis set).

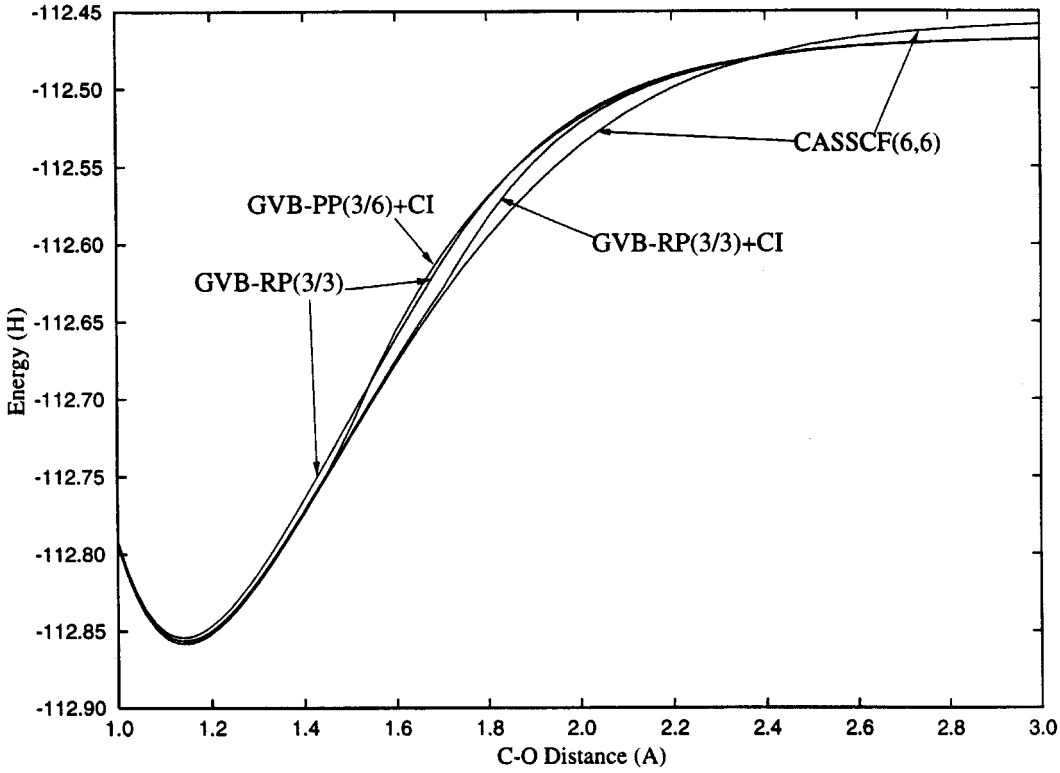

FIGURE 4. CO dissociation potential at various levels of theory. GVB–RP + CI (GVB–RP followed by active space CI) shows that GVB-RP selects the optimal active space in a broader region than GVB–PP.

qualitatively correct description of the reaction barrier. GVB–RP performs as well as UHF, predicting a barrier approximately 7 kcal/mol higher than CASSCF. The GVB-PP potential has a somewhat higher barrier.

Forbidden Reaction: $H_2 + H_2$

The next reaction we studied is $H_2 + H_2$ with D_{2h} (rectangular planar) geometry. The reaction coordinate was determined at the CASSCF(4, 4) level with 6-31G** basis set, and it is reported in Figure 8. The same reaction coordinate was then used for all levels of theory. The reaction profiles are reported in Figure 9. In the UHF case, only the singlet spin state was considered.

As shown in Figure 9, UHF and GVB–PP fail to describe properly the transition state. The MP2 treatment of the UHF wave function does not correct the problem. The GVB–RP potential energy profile is not smooth, that is, it is the superposition of two distinct electronic states with a discontinuity in the gradient; however, the discontinuity is not at the transition state, and we expect the GVB–RP description to provide good potential energy surfaces for most transition states. GVB–RP fails to describe the transition-state region when it is important to include configurations to describe charge transfer from one pair to another, as is the case for *tight* transition states, with all the active electrons confined in a restricted volume of space. In this case it is easy to include the missing configurations at the post-SCF level.

Forbidden Reaction: Cyctobutadiene

In order to understand the importance of this shortcoming, we studied the transition between the two forms of cyclobutadiene:

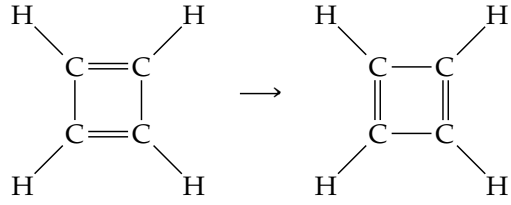

The reaction coordinate was determined at the CASSCF(4, 4) level, with correlation on the four π

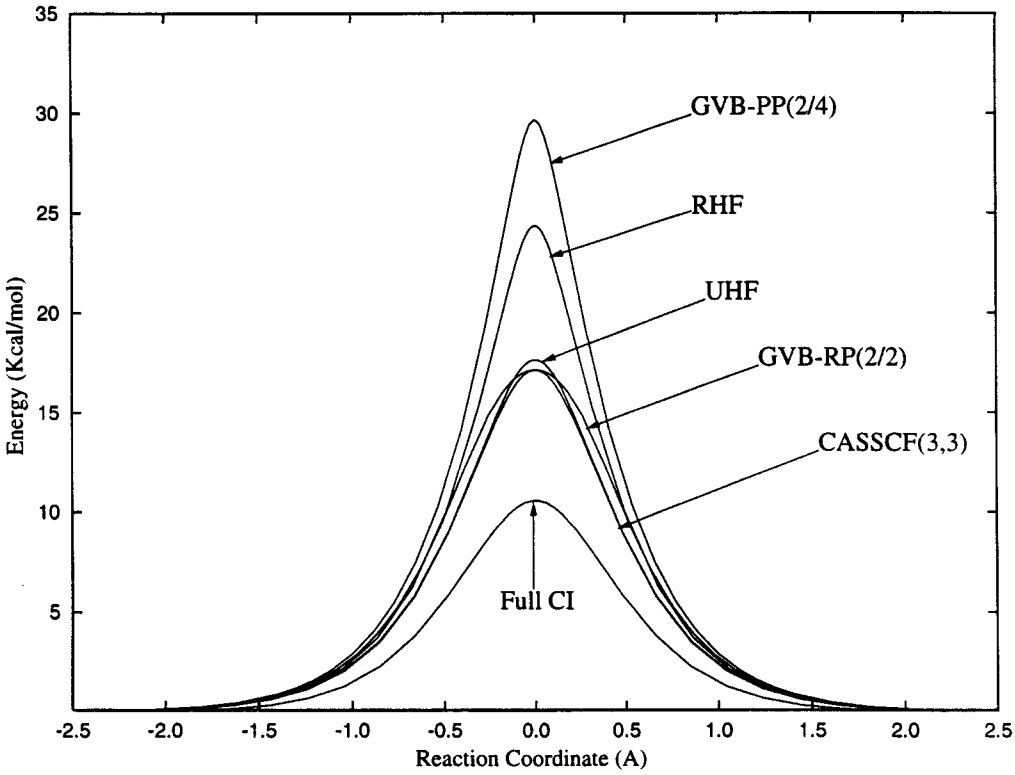

FIGURE 5. Energy profile for $H_2 + H \rightarrow H + H_2$ along the reaction path (using cc-pVTZ basis set). The reaction coordinate was determined for each level of theory as reported in Figure 6, with the exception of full CI, which is based on the CASSCF reaction coordinate.

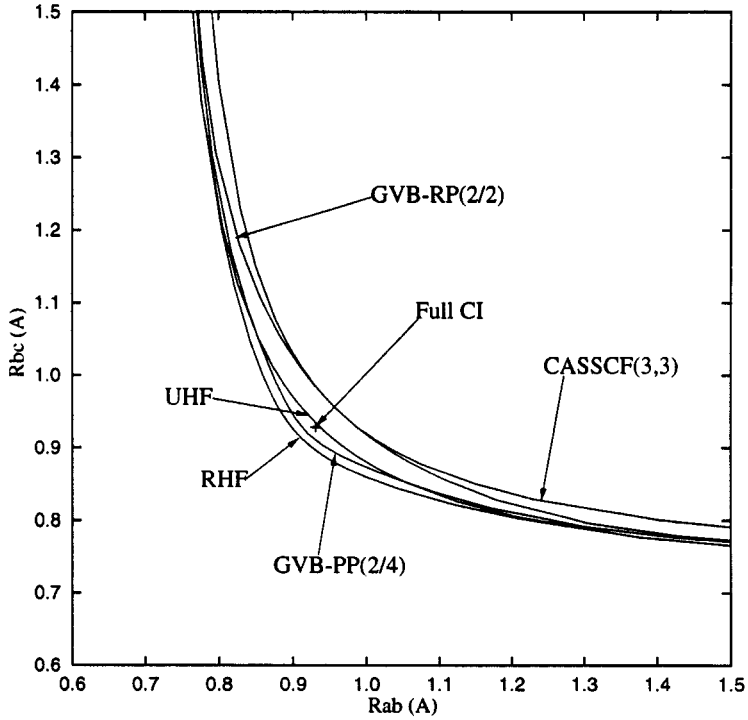

FIGURE 6. Reaction coordinate for $H_aH_b + H_c \rightarrow H_a + H_bH_c$ for various levels of theory (using the cc-pVTZ basis set). The full CI transition state is included for comparison.

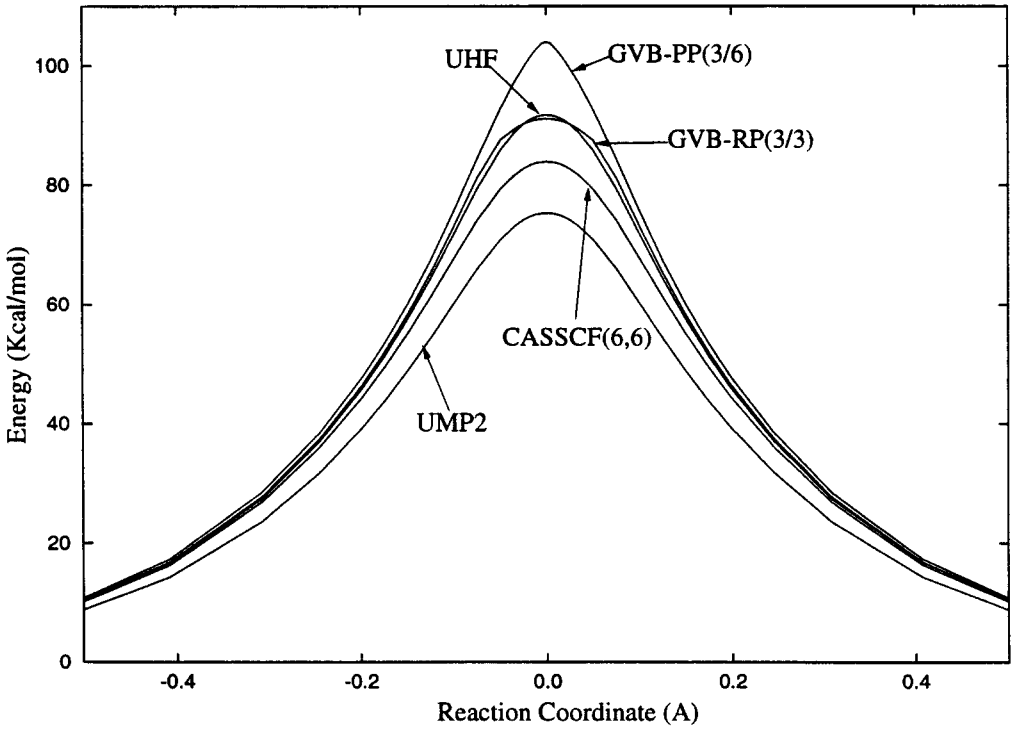

FIGURE 7. Energy profile for $H_2 + H_2 + H_2$ (D_{3h} geometry) along the reaction path. The reaction coordinate was determined at the MP2 level of theory.

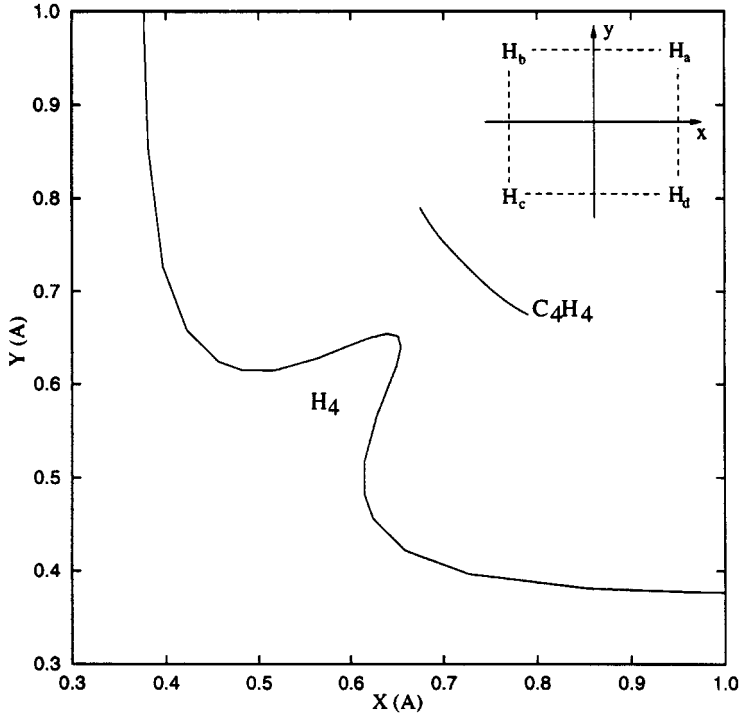

FIGURE 8. Reaction coordinates for pseudorotation of C_4H_4 and for the transition state of $H_aH_b + H_cH_d \rightarrow H_aH_d + H_bH_c$. Both curves are computed at CASSCF(4, 4) level and refer to D_{2h} systems. H_4 refers to the position of H_a in the plane of the molecule as depicted in the upper right corner. C_4H_4 refers to the position of one of the cyclobutadiene carbons. Notice that cyclobutadiene cannot stretch at the transition state due to the presence of the σ bonds.

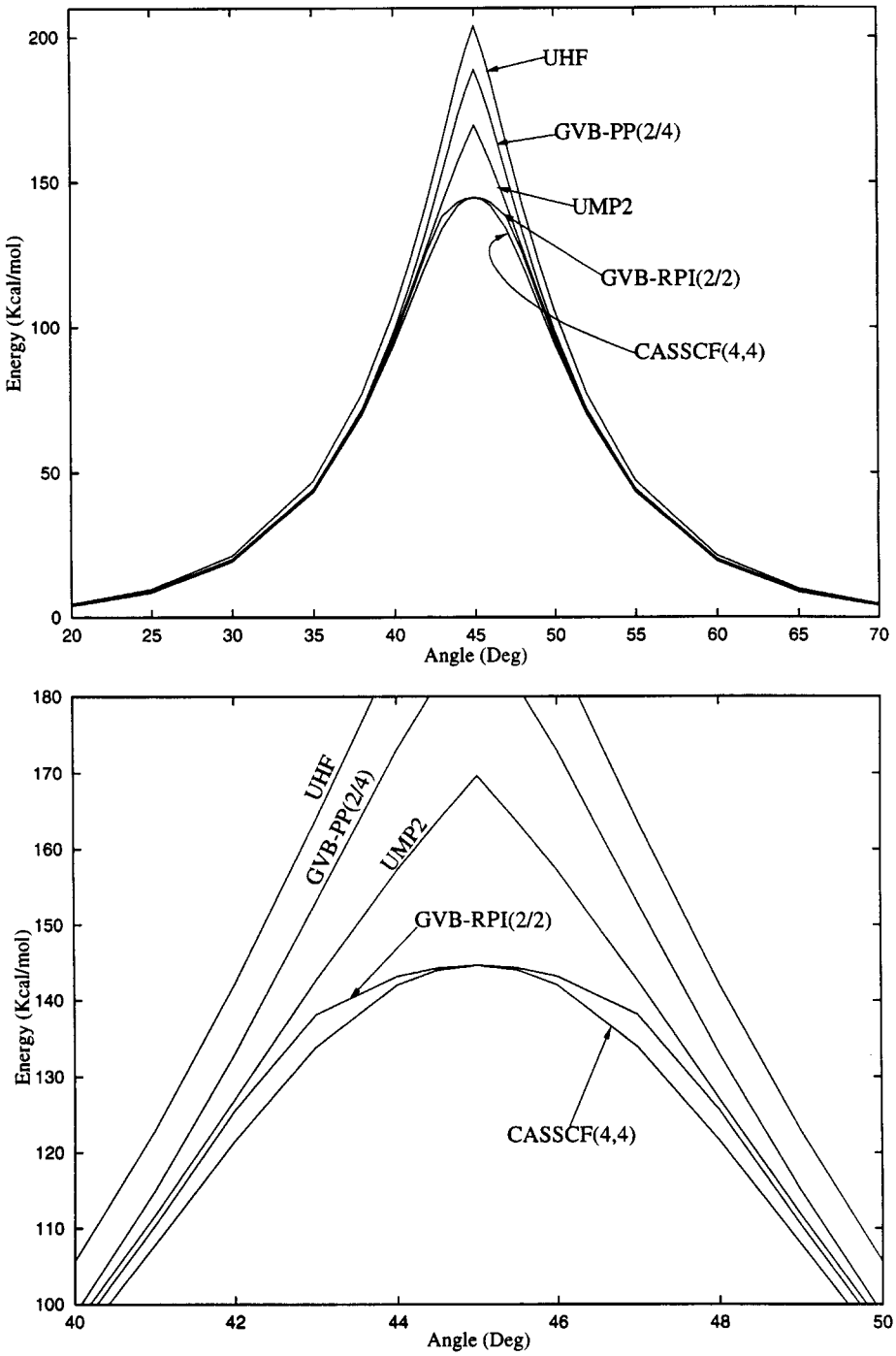

FIGURE 9. Energy profile for $H_2 + H_2$ (D_{2h} geometry) along the CASSCF(4, 4) reaction coordinate reported in Figure 8 (H_4). The abscissa is the angle arctan(Y/X), where X and Y are the Cartesian coordinates of Figure 8. The bottom plot is a magnification of the transition state region reported on the top. The GVB–RP potential has an edge at about 43° and 47°.

electrons, using 6-31G* basis set and was used for all levels of theory. The reaction coordinate is reported in Figure 8 along with the reaction coordinate for $H_2 + H_2$ reaction. The main difference between the two paths is that in the case of cyclobutadiene the transition state cannot stretch outward due to the presence of the σ bonds.

As reported in Figure 10, UHF, UHF + MP2, GVB–PP, and GVB–RP fail to describe the transition properly, while CASSCF provides a physically reasonable potential energy profile.

A detailed analysis of the wave function indicates that the difference between GVB–RP and CASSCF wave functions is due to two configurations, shown schematically in Figure 11. Inclusion of the extra configurations at the post-SCF level lowers the GVB–RP energy to within 0.4 kcal/mol of the CASSCF energy. This indicates that the active space selected by GVB–RP is almost optimal.

This potential energy is compared with CASSCF in Figure 12.

TRANSITION-METAL COMPOUNDS

As an example of reaction at a transition-metal center, we studied the H insertion into the Ru = CH_2 double bond in the complex $ClRuHCH_2 \rightarrow ClRuCH_3$.

The reaction coordinate determined at the UHF + MP2 level was used also for the other levels of theory. [We used 6-31G** basis set on the carbon and hydrogens, Los Alamos Core-Valence (LACV) effective core potential (ECP) and double-ζ basis set on Ru, and LAV ECP and double-ζ basis set on Cl.] Figure 13 summarizes the results obtained at various levels. The active space used to describe the reaction includes six electrons and six orbitals in the H–Ru–C plane. These orbitals correspond to the σ_{RuH}, σ^*_{RuH}, σ_{RuC}, σ^*_{RuC}, π_{RuC}, and π^*_{RuC} in

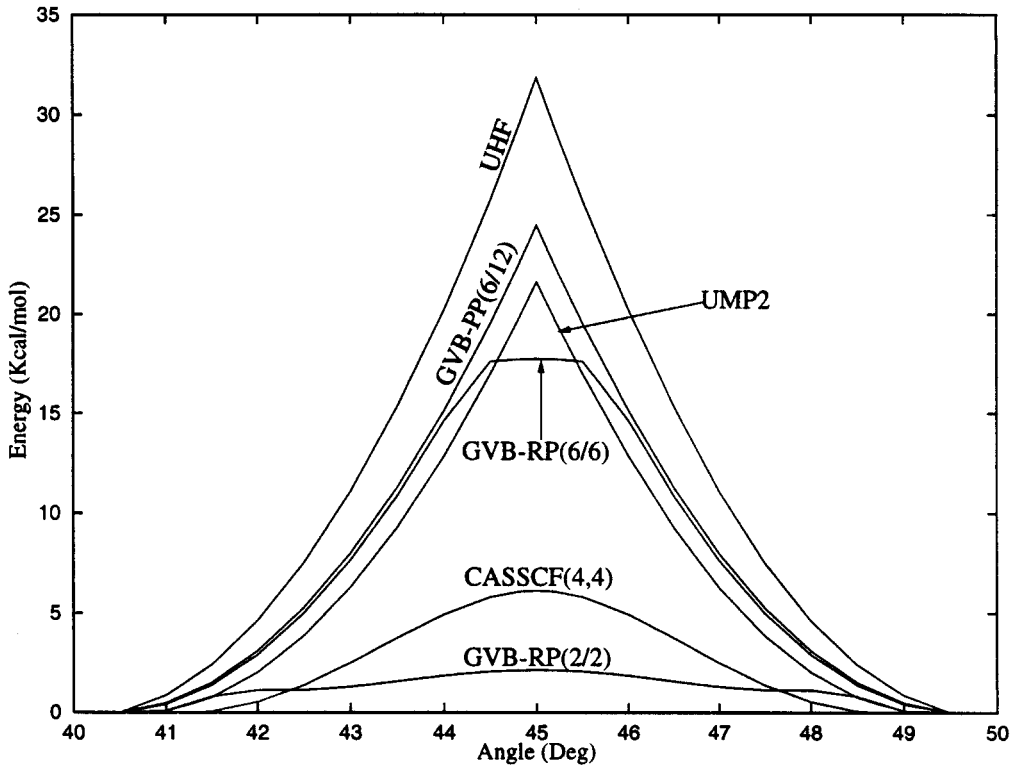

FIGURE 10. Energy profile along the CASSCF(4, 4) reaction coordinate for pseudorotation of C_4H_4 reported in Figure 8 (C_4H_4).

Orbitals

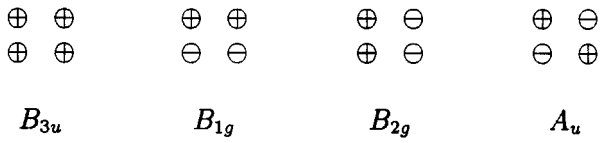

Configurations

Config. N.	Occupancy			
	B_{3u}	B_{1g}	B_{2g}	A_u
1	2	2	0	0
2	2	0	2	0
3	0	2	0	2
4	0	0	2	2
5	1	1	1	1
6	0	2	2	0
7	2	0	0	2

FIGURE 11. Decomposition of the active space for C_4H_4. The four symmetry orbitals are represented on top; each circle represents the lobe of a p orbital coming out of the page and the sign represents its phase. The bottom reports the configurations important for the CASSCF wave function. Configurations 1–5 form the GVB–RP active space. When configurations 6 and 7 are added to GVB–RP with a post-SCF CI, the resulting energies approach the CASSCF result as reported in Figure 12.

the reactant and to σ_{RuC}, σ^*_{RuC}, σ_{CH}, σ^*_{CH}, and two d orbitals on Ru in the product.

While UHF cannot describe properly the reactants and predicts essentially no barrier for the forward reaction, all other methods give a more reasonable description. Figure 13 shows clearly that although the GVB–PP description is qualitatively correct, this level of theory cannot be trusted in the quantitative estimate of reaction and activation enthalpies.

GVB–RP provides a substantially better result, recovering a large portion of the active-space correlation energy (95.7, 89.7, and 94.5% of the active space correlation energy is recovered at 25°, 53°, and 90°, respectively). CASSCF and UMP2 are provided for comparison.

COST

To compare the cost of GVB–RP with other self-consistent methods, we studied the N_2 molecule (6-31G* basis set, experimental geometry) with correlation on up to five pairs of electrons.

The code for CASSCF and for GVB–RP could be run only using different algorithms to compute the integrals, so a direct comparison of the absolute timings would not be meaningful. Instead we report in Figure 14 the cost of each SCF iteration relative to one HF iteration. Each self-consistent method is thus compared with a HF computation based on the same technique to evaluate the integrals.

From Figure 14 it is apparent that GVB–PP, GVB–RP, and CASSCF are slightly more expensive than HF for up to six active electrons (or three GVB pairs). As more electrons are included in the active space, CASSCF becomes considerably more expensive than GVB–RP. This is due to the nontractable scaling of CASSCF with the size of the active space.

To study the scaling with respect to both the number of basis functions and the number of active electrons, we carried out computations on systems formed with one to five acetylene molecules [$(HCCH)_n$, $n = 1, \ldots, 5$]. The range of parameters spanned is of 22–110 basis functions, 3–12 GVB–PP pairs, and 3–9 GVB–RP pairs.

Using our code, the cost of HF, GVB-PP, and GVB–RP is fit by the following equations (N = number of basis functions; P = number of GVB pairs):

$$\begin{aligned} \text{HF} &= \alpha N^4, \\ \text{GVB–PP} &= 0.70\alpha N^4(P+1), \quad (P \geq 1), \\ \text{GVB–RP} &= 0.47\alpha N^4 P(P+1), \quad (P \geq 2), \end{aligned}$$

where $\alpha = 2.71 \cdot 10^{-7}$ sec/iteration on a HP 9000/735 workstation running at 99 MHz.

COMPUTATIONAL DETAILS

All RHF, GVB–PP, GVB–RP, full CI computations, as well as the CASSCF for the Ru system were performed with our code. All UHF, UMP2, and the remaining CASSCF computations were performed using GAUSSIAN92 and GAUSSIAN94 [8].

Conclusions

We have developed a self-consistent computational method, called GVB–RP, which is able to

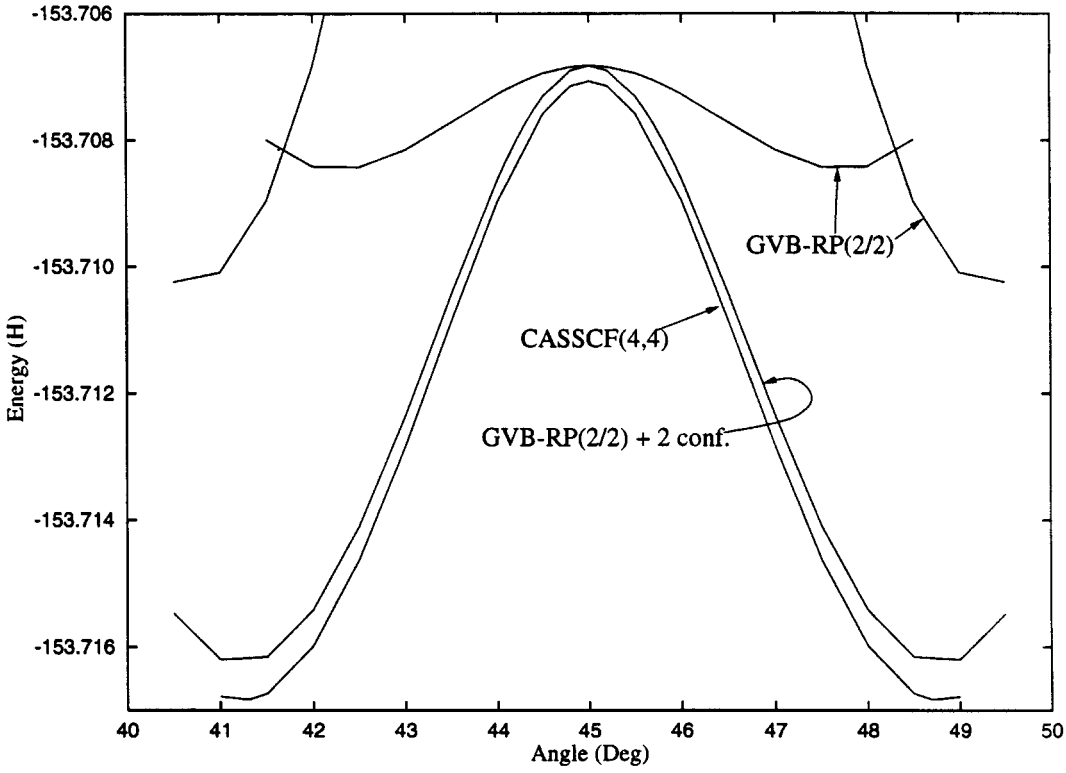

FIGURE 12. Energy profile obtained when two extra configurations are added at the post-SCF stage to the GVB–RP wavefunction is reported as GVB–RP(2/2) + 2 conf. Notice that the GVB–RP(2/2) leads to two energy surfaces depending on spin coupling.

provide good potential energy surfaces for most reactions that are not properly described at the HF or GVB–PP levels. The method considers only a small number of selected configurations to describe the wave function and requires the transformation of a limited number of integrals at each self-consistent step.

We tested GVB–RP on a few simple systems to verify its reliability, test its limits, and suggest possible improvements at the post-SCF level.

The potential energies obtained are qualitatively correct for most chemical processes. In particular, GVB–RP performs better than HF or GVB–PP for the description of multiple-bond dissociations, often approaching the CASSCF quality. GVB–RP describes correctly the transition states for radical and allowed reactions. Although GVB–RP does not describe forbidden reactions with a regular energy profile, it can describe correctly both the reactants and the transition state. It also proves a powerful method to select the correct active space in the case of transition-metal systems, where correlation between several electrons in the same region of space is important.

GVB–RP is considerably less expensive than CASSCF for systems with large active spaces.

Appendix

It is necessary to optimize three kinds of CI coefficients:

- Pair coefficients C_I^s, C_I^u, defined in Eq. (2), for all GVB pairs I.
- Spin coefficients C_{IJ}^s, C_{IJ}^t, defined in Eq. (3), for all combinations IJ.
- CI coefficients C_0, C_{IJ}, defined in Eq. (5).

We optimize each kind of coefficient assuming the other kinds to be fixed and iterate to a self-consistent convergence.

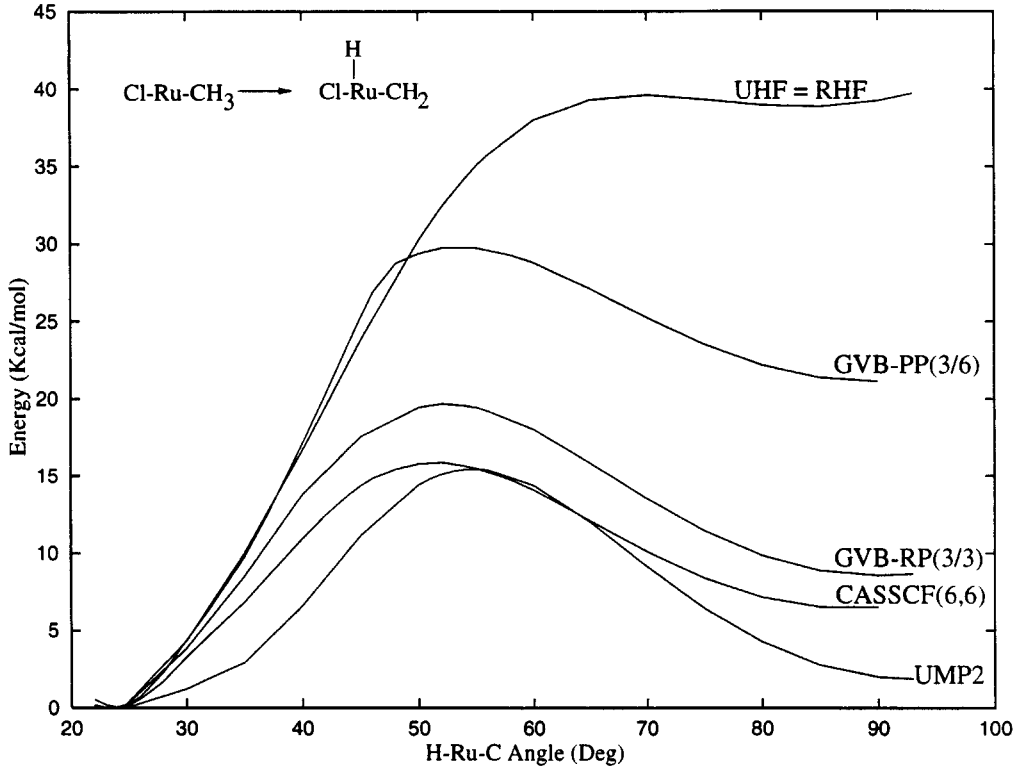

FIGURE 13. Energy profile for $ClHRuCH_2 \rightarrow ClRuCH_3$ at various levels of theory.

PAIR COEFFICIENTS

Consider the GVB coefficients for a pair $P \in \mathrm{RP}$, namely $C_p = C_P^g$ and $C_{p'} = C_P^u$. Assuming that all other parameters are fixed, the total energy can be expressed as

$$\begin{aligned} E = \text{constant} &+ 2f_p h_p + 2f_{p'} h_{p'} + a_{pp} J_{pp} + b_{pp} K_{pp} \\ &+ a_{p'p'} J_{p'p'} + b_{p'p'} K_{p'p'} \\ &+ 2 \sum_{i \notin P} (a_{ip} J_{ip} + b_{ip} K_{ip} + a_{ip'} J_{ip'} + b_{ip'} K_{ip'}) \\ &+ 2(a_{pp'} J_{pp'} + b_{pp'} K_{pp'}) \\ &+ \sum_{I \neq P} [\, r_{IP}(ip|i'p') + s_{IP}(ip'|i'p) + t_{IP}(ii'|pp')]. \end{aligned}$$

Substituting the values of the parameters f, a, b, r, s, and t and collecting the pair coefficients, this becomes

$$\tfrac{1}{2}E = \tilde{\mathbf{C}}\mathbf{Y}\mathbf{C} - 2\tilde{\mathbf{C}}\mathbf{X} + \text{constant}$$

where

$$\mathbf{C} = \begin{vmatrix} C_p \\ C_{p'} \end{vmatrix}, \qquad \mathbf{Y} = \begin{vmatrix} Y_{pp} & Y_{pp'} \\ Y_{p'p} & Y_{p'p'} \end{vmatrix}, \qquad \mathbf{X} = \begin{vmatrix} X_p \\ X_{p'} \end{vmatrix}.$$

The explicit values of each element are

$$\begin{aligned} Y_{pp} &= \Gamma_P h_p + \tfrac{1}{2}\Gamma_P J_{pp} + \Gamma_P \sum_{i \notin \mathrm{RP}} (2f_i J_{ip} - f_i K_{ip}) \\ &\quad + \sum_{i \in \mathrm{RP},\, i \notin P} \Big\{ \big[(\Gamma_I + \Gamma_P + C_{IP}^2 - 1) C_i^2 \\ &\quad + \tfrac{1}{2}(1 - \Gamma_I - C_{IP}^2) \big] (2J_{ip} - K_{ip}) \Big\}, \\ Y_{p'p'} &= \Gamma_P h_{p'} + \tfrac{1}{2}\Gamma_P J_{p'p'} + \Gamma_P \sum_{i \notin \mathrm{RP}} (2f_i J_{ip'} - f_i K_{ip'}) \\ &\quad + \sum_{i \in \mathrm{RP},\, i \notin P} \Big\{ \big[(\Gamma_I + \Gamma_P + C_{IP}^2 - 1) C_i^2 \\ &\quad + \tfrac{1}{2}(1 - \Gamma_I - C_{IP}^2) \big] (2J_{ip'} - K_{ip'}) \Big\}, \\ Y_{p'p} &= Y_{pp'} = -\tfrac{1}{2}\Gamma_P K_{pp'}, \end{aligned}$$

$$X_p = -\tfrac{1}{4}\sum_{I\neq P}\Bigg\{\Big[C_0C_{IP}C_{i'}\big(\sqrt{3}\,C^t_{IP}+C^s_{IP}\big) - C_i\sum_K C_{IK}C_{KP}(C^s_{IK}C^s_{KP}+C^t_{IK}C^t_{KP})\Big](ip|i'p') + \Big[C_0C_{IP}C_i\big(\sqrt{3}\,C^t_{IP}-C^s_{IP}\big) + C_{i'}\sum_K C_{IK}C_{KP}(C^s_{IK}C^s_{KP}-C^t_{IK}C^t_{KP})\Big](ip'|i'p) + \Big[2C_0C_{IP}(C_i-C_{i'})C^s_{IP} + 2(C_i-C_{i'})\sum_K C_{IK}C_{KP}(C^s_{IK}C^s_{KP})\Big](ii'|pp')\Bigg\},$$

$$X_{p'} = -\tfrac{1}{4}\sum_{I\neq P}\Bigg\{\Big[C_0C_{IP}C_i\big(\sqrt{3}\,C^t_{IP}+C^s_{IP}\big) - C_{i'}\sum_K C_{IK}C_{KP}(C^s_{IK}C^s_{KP}+C^t_{IK}C^t_{KP})\Big](ip|i'p') + \Big[C_0C_{IP}C_{i'}\big(\sqrt{3}\,C^t_{IP}-C^s_{IP}\big) + C_i\sum_K C_{IK}C_{KP}(C^s_{IK}C^s_{KP}-C^t_{IK}C^t_{KP})\Big]\times(ip'|i'p) - \Big[2C_0C_{IP}(C_i-C_{i'})C^s_{IP} + 2(C_i-C_{i'})\sum_K C_{IK}C_{KP}(C^s_{IK}C^s_{KP})\Big](ii'|pp')\Bigg\}.$$

We minimize the energy subject to the constraint $\tilde{\mathbf{C}}\mathbf{C} = 1$:

$$\frac{\partial[\tilde{\mathbf{C}}\mathbf{Y}\mathbf{C} - 2\tilde{\mathbf{C}}\mathbf{X} + \text{constant} - \lambda(\tilde{\mathbf{C}}\mathbf{C}-1)]}{\partial\mathbf{C}} \propto (\mathbf{Y}-\lambda\mathbf{I})\mathbf{C} - \mathbf{X} = 0,$$

where λ is the Lagrange multiplier.

The system has solution

$$\mathbf{C} = \begin{vmatrix} C_p \\ C_{p'} \end{vmatrix} = \begin{vmatrix} Y_{pp}-\lambda & Y_{pp'} \\ Y_{p'p} & Y_{p'p'}-\lambda \end{vmatrix}^{-1} \begin{vmatrix} X_p \\ X_{p'} \end{vmatrix}$$

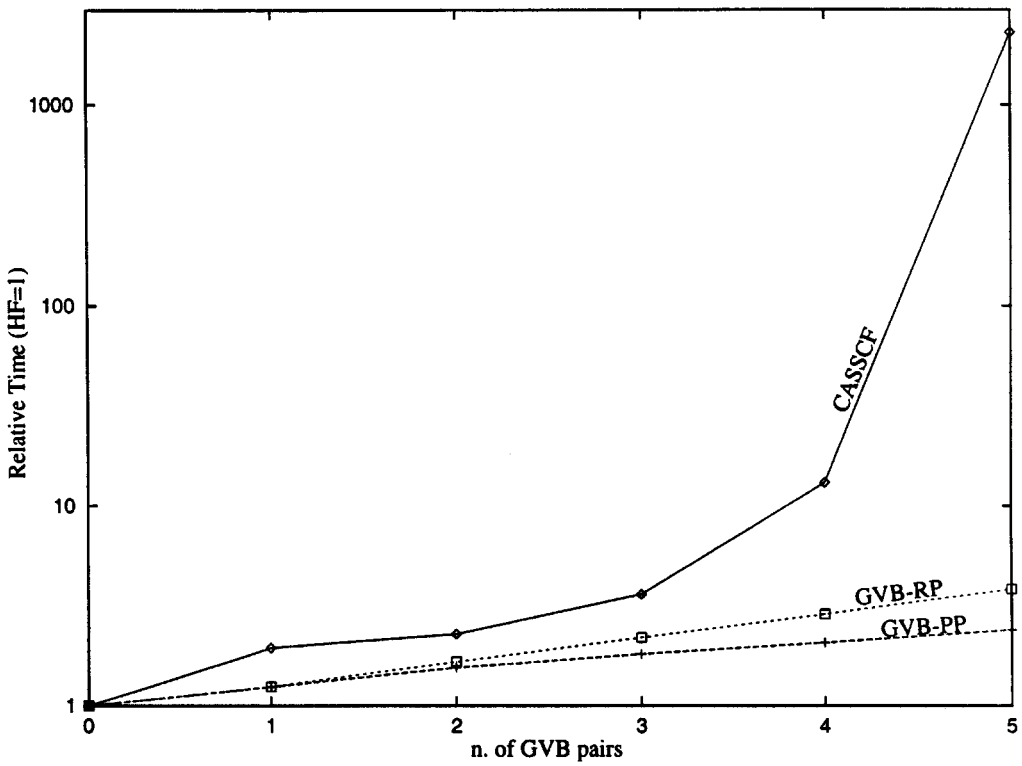

FIGURE 14. Cost of self-consistent correlated methods relative to HF. The results refer to the N_2 molecule with 6-31G* basis set at experimental geometry. One GVB pair corresponds to two active electrons and two orbitals. The CASSCF value for five GVB pairs (10 electrons, 10 orbitals) is approximately 2300, based on a computation run on a different computer.

$$= \frac{1}{(Y_{pp} - \lambda)(Y_{p'p'} - \lambda) - Y_{p'p}^2} \times \begin{vmatrix} Y_{p'p'} - \lambda & -Y_{pp'} \\ -Y_{p'p} & Y_{pp} - \lambda \end{vmatrix} \begin{vmatrix} X_p \\ X_{p'} \end{vmatrix}$$

$$= \frac{1}{(Y_{pp} - \lambda)(Y_{p'p'} - \lambda) - Y_{p'p}^2} \times \begin{vmatrix} (Y_{p'p'} - \lambda) X_p - Y_{pp'} X_{p'} \\ (Y_{pp} - \lambda) X_{p'} - Y_{p'p} X_p \end{vmatrix},$$

which leads to the normalization condition

$$1 = C_p^2 + C_{p'}^2 = \frac{[(Y_{p'p'} - \lambda) X_p - Y_{pp'} X_{p'}]^2 + [(Y_{pp} - \lambda) X_{p'} - Y_{p'p} X_p]^2}{[(Y_{pp} - \lambda)(Y_{p'p'} - \lambda) - Y_{p'p}^2]^2},$$

which in turn leads to the equation in λ

$$\begin{aligned} 0 = {} & \lambda^4 - 2Tr\lambda^3 + \left[2\Delta + Tr^2 - X_{p'}^2 - X_p^2\right]\lambda^2 \\ & + \left[2(X_p Y_{p'p'} - Y_{pp'} X_{p'}) X_p \right. \\ & \left. + 2(X_{p'} Y_{pp} - Y_{pp'} X_p) X_{p'} - 2\Delta Tr\right]\lambda \\ & - (X_p Y_{p'p'} - Y_{pp'} X_{p'})^2 + \Delta^2 \\ & - (X_{p'} Y_{pp} - Y_{pp'} X_p)^2, \end{aligned}$$

where

$$\Delta = Y_{pp} Y_{p'p'} - Y_{pp'}^2, \qquad Tr = Y_{pp} + Y_{p'p'},$$

which has four real solutions since the Hamiltonian is hermitian.

The λ term is related to the energy by $E \propto \lambda - \tilde{\mathbf{C}}\mathbf{X}$, which enables us to select the solution that minimizes the energy. Notice that the normalization condition can be satisfied in all cases except when λ is an eigenvalue of the matrix $\mathbf{Y}$, in which case it must be $\mathbf{X} = 0$, and we can solve the homogeneous equation.

The optimal coefficients for each pair depend on the coefficients of the other pairs and on the other CI coefficients; therefore, the solution must be determined iteratively until self-consistency.

In the special case that pair P is treated at the perfect pairing level, the above expressions simplify as follows.

The total energy can be expressed as

$$\begin{aligned} E = {} & \text{constant} + 2f_p h_p + 2f_{p'} h_{p'} + a_{pp} J_{pp} + b_{pp} K_{pp} \\ & + a_{p'p'} J_{p'p'} + b_{p'p'} K_{p'p'} \\ & + 2 \sum_{i \notin P} (a_{ip} J_{ip} + b_{ip} K_{ip} + a_{ip'} J_{ip'} + b_{ip'} K_{ip'}) \\ & + 2(a_{pp'} J_{pp'} + b_{pp'} K_{pp'}), \end{aligned}$$

which takes the form

$$\tfrac{1}{2} E = \text{constant} + \tilde{\mathbf{C}}\mathbf{Y}\mathbf{C},$$

where

$$\mathbf{C} = \begin{vmatrix} C_p \\ C_{p'} \end{vmatrix} \quad \text{and} \quad \mathbf{Y} = \begin{vmatrix} Y_{pp} & Y_{pp'} \\ Y_{p'p} & Y_{p'p'} \end{vmatrix},$$

and

$$\begin{aligned} Y_{ii} &= h_i + \tfrac{1}{2} J_{ii} + \sum_{j \notin P} f_j (2J_{ji} - K_{ji}), \\ Y_{ij} &= -\tfrac{1}{2} K_{ij}, \quad \text{for } i \neq j. \end{aligned}$$

We minimize the energy with the constraint $\tilde{\mathbf{C}}\mathbf{C} = 1$:

$$\frac{\partial[\tilde{\mathbf{C}}\mathbf{Y}\mathbf{C} - \lambda(\tilde{\mathbf{C}}\mathbf{C} - 1)]}{\partial \mathbf{C}} \propto \mathbf{Y}\mathbf{C} - \lambda\mathbf{C} = 0.$$

In this case λ is directly proportional to the energy.

SPIN COEFFICIENTS

We optimize the coefficients C_{PQ}^t and C_{PQ}^s assuming all other coefficients are frozen.

All terms in the energy expression that do not depend on C_{PQ}^t or C_{PQ}^s are constant, so we can write:

$$\begin{aligned} E = {} & \text{constant} + 2b_{pp'} K_{pp'} + 2b_{pq} K_{pq} + 2b_{pq'} K_{pq'} \\ & + 2b_{p'q} K_{p'q} + 2b_{p'q'} K_{p'q'} + 2b_{qq'} K_{qq'} \\ & + 2r_{PQ}(pq|p'q') + 2s_{PQ}(pq'|p'q) \\ & + 2t_{PQ}(pp'|qq') \\ & + 2 \sum_{I \neq P,Q} \left[r_{IP}(ip|i'p') + s_{IP}(ip'|i'p) \right. \\ & + t_{IP}(ii'|pp') + r_{IQ}(iq|i'q') \\ & \left. + s_{IQ}(iq'|i'q) + t_{IQ}(ii'|qq') \right], \end{aligned}$$

which is put in the form

$$E = \text{constant} + \tilde{\mathbf{C}}\mathbf{Y}\mathbf{C} - 2\tilde{\mathbf{C}}\mathbf{X},$$

where

$$\begin{aligned}
Y_{tt} &= C_{PQ}^2\left[\tfrac{1}{2}(K_{pq} + K_{pq'} + K_{p'q} + K_{p'q'}) - (K_{pp'} + K_{qq'})\right],\\
Y_{ss} &= C_{PQ}^2\left[(K_{pp'} + K_{qq'}) - \tfrac{1}{2}(K_{pq} + K_{pq'} + K_{p'q} + K_{p'q'})\right],\\
Y_{st} &= Y_{ts} = C_{PQ}^2\frac{\sqrt{3}}{2}(K_{pq} + K_{p'q'} - K_{pq'} - K_{p'q}),\\
X_t &= -\sqrt{3}\,C_0C_{PQ}(C_pC_{q'} + C_{p'}C_q)(pq|p'q')\\
&\quad -\sqrt{3}\,C_0C_{PQ}(C_pC_q + C_{p'}C_{q'})(pq'|p'q)\\
&\quad + C_{PQ}\sum_{I\neq P,\,Q}\left[C_{IQ}C_{IQ}^t(C_iC_p + C_{i'}C_{p'})(ip|i'p')\right.\\
&\quad + C_{IQ}C_{IQ}^t(C_iC_{p'} + C_{i'}C_p)(ip'|i'p)\\
&\quad + C_{IP}C_{IP}^t(C_iC_q + C_{i'}C_{q'})(iq|i'q')\\
&\quad \left. + C_{IP}C_{IP}^t(C_iC_{q'} + C_{i'}C_q)(iq'|i'q)\right],\\
X_s &= -C_0C_{PQ}(C_pC_{q'} + C_{p'}C_q)(pq|p'q')\\
&\quad + C_0C_{PQ}(C_pC_q + C_{p'}C_{q'})(pq'|p'q)\\
&\quad - 2C_0C_{PQ}(C_p - C_{p'})(C_q - C_{q'})(pp'|qq')\\
&\quad + C_{PQ}\sum_{I\neq P,\,Q}\left[C_{IQ}C_{IQ}^s(C_iC_p + C_{i'}C_{p'})(ip|i'p')\right.\\
&\quad - C_{IQ}C_{IQ}^s(C_iC_{p'} + C_{i'}C_p)(ip'|i'p)\\
&\quad - 2C_{IQ}C_{IQ}^s(C_i - C_{i'})(C_p - C_{p'})(ii'|pp')\\
&\quad + C_{IP}C_{IP}^s(C_iC_q + C_{i'}C_{q'})(iq|i'q')\\
&\quad - C_{IP}C_{IP}^s(C_iC_{q'} + C_{i'}C_q)(iq'|i'q)\\
&\quad \left. - 2C_{IP}C_{IP}^s(C_i - C_{i'})(C_q - C_{q'})(ii'|qq')\right],
\end{aligned}$$

and the optimal coefficients can be found using the same algorithm described in the pair coefficient optimization (this time the $\mathbf{Y}$ matrix is traceless; therefore, the equation in λ is simpler).

CI COEFFICIENTS

Let $\mathbf{H}$ denote the CI matrix:

$$\mathbf{H} = \begin{vmatrix}
\langle\Psi^{\mathrm{GVB}}|H|\Psi^{\mathrm{GVB}}\rangle & \langle\Psi^{\mathrm{GVB}}|H|\Psi_{12}^{\mathrm{RP}}\rangle & \langle\Psi^{\mathrm{GVB}}|H|\Psi_{13}^{\mathrm{RP}}\rangle & \cdots & \Psi^{\mathrm{GVB}}|H|\Psi_{R-1,\,R}^{\mathrm{RP}}\rangle\\
\langle\Psi_{12}^{\mathrm{RP}}|H|\Psi^{\mathrm{GVB}}\rangle & \langle\Psi_{12}^{\mathrm{RP}}|H|\Psi_{12}^{\mathrm{RP}}\rangle & \langle\Psi_{12}^{\mathrm{RP}}|H|\Psi_{13}^{\mathrm{RP}}\rangle & \cdots & \langle\Psi_{12}^{\mathrm{RP}}|H|\Psi_{R-1,\,R}^{\mathrm{RP}}\rangle\\
\langle\Psi_{13}^{\mathrm{RP}}|H|\Psi^{\mathrm{GVB}}\rangle & \langle\Psi_{13}^{\mathrm{RP}}|H|\Psi_{12}^{\mathrm{RP}}\rangle & \langle\Psi_{13}^{\mathrm{RP}}|H|\Psi_{13}^{\mathrm{RP}}\rangle & \cdots & \langle\Psi_{13}^{\mathrm{RP}}|H|\Psi_{R-1,\,R}^{\mathrm{RP}}\rangle\\
\vdots & \vdots & \vdots & \ddots & \vdots\\
\langle\Psi_{R-1,\,R}^{\mathrm{RP}}|H|\Psi^{\mathrm{GVB}}\rangle & \langle\Psi_{R-1,\,R}^{\mathrm{RP}}|H|\Psi_{12}^{\mathrm{RP}}\rangle & \langle\Psi_{R-1,\,R}^{\mathrm{RP}}|H|\Psi_{13}^{\mathrm{RP}}\rangle & \cdots & \langle\Psi_{R-1,\,R}^{\mathrm{RP}}|H|\Psi_{R-1,\,R}^{\mathrm{RP}}\rangle
\end{vmatrix}.$$

Each element of $\mathbf{H}$ can be expressed as function of the pair and spin coefficients by expanding each bra and ket and collecting equal integrals over the orbitals.

The ground-state CI coefficients are given by the eigenvector with lowest eigenvalue, i.e., lowest energy, of the above matrix.

Again, the matrix elements depend on the pair and spin coefficients, which in turn depend on the CI coefficients, so a self-consistent approach is required.

ACKNOWLEDGMENTS

We thank Richard P. Muller for working out the detailed formulas for a special case. This research was supported by ASF (ASC 92-17368 and CHE 95-22179). In addition, the facilities of the MSC are also supported by grants from ARO/DURIP, BP Chemical, ARO, Exxon, Seiko-Epson Owens Corning, Asahi Chemical, Saudi Aramco, Beckman Institute, Chevron Petroleum Technology Co., Chevron Chemical Co., NASA/Ames, NASA/JPL, ONR, Avery Dennison, and Chevron Research Technology Co.

References

1. Hinze, J. J Chem Phys 1973, 59, 6424. Shepard, .R.; Adv Chem Phys 1987, 69, 63.
2. McWeeny, R. Methods of Molecular Quantum Mechanics, 2nd ed., Academic: San Diego, 1992.

3. Roos, B. O.; Taylor, P. R.; Siegbahn, P. E. M. Chem Phys 1980, 48, 157. Roos, B. O. Adv Chem Phys 1987, 69, 399.
4. Szabo, A.; Ostlund, N. S. Modern Quantum Chemistry, McGraw-Hill: New York, 1989.
5. Bobrowicz, F. W.; Goddard III, W. A. Modern Theoretical Chemistry, Vol. 3, Methods of Electronic Structure Theory; Shaefer, H. F. III, Ed.; Plenum: New York, 1977.
6. See, for instance, Carter, E. A.; Goddard III, W. A. J. Chem Phys 1988, 88, 3132; J Chem Phys 1988, 88, 3132.
7. Lofthus, A.; Krupenie, P. H. J. Phys Chem Ref Data 1977, 6, 113.
8. Frisch, M. J.; Trucks, G. W.; Schlegel, H. B.; Gill, P. M. W.; Johnson, B. G.; Wong, M. W.; Foresman, J. B.; Robb, M. A.; Head-Gordon. M.; Replogle, E. S.; Gomperts, R.; Andres, J. L.; Raghavachari, K.; Binkley, J. S.; Gonzalez, C.; Martin, R. L.; Fox, D. J.; Defrees, D. J.; Baker, J.; Stewart, J. P. P; Pople, J. A.; Gaussian, Inc., Pittsburgh, PA, 1993. Gaussian 92/DFT, Revision F.4, Frich, M. J.; Trucks, G. W.; Schlegel, H. B.; Gill, P. M. W.; Johnson, B. G.; Robb, M. A.; Cheeseman, J. R.; Keith, T.; Petersson, G. A.; Montgomery, J. A.; Raghavachari, K.; Al-Laham, M. A.; Zakrewski, V. G; Ortiz, J. V.; Foresman, J. B.; Peng, C. Y.; Ayala, P. Y.; Chen, W.; Wong, M. W.; Andres, J. L.; Replogle, E. S.; Gomperts. R.; Martin, R. L.; Fox, D. J.; Binkley, J. S.; DeRees, D. J.; Baker, J.; Stewart, J. P. P; Head-Gordon, M.; Gonzalez, C.; Pople, J. A. Gaussian 94, Revision B.3, Gaussian, Inc., Pittsburgh, PA, 1995.